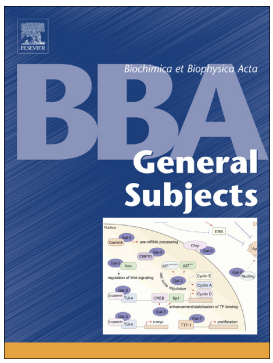

Mechanistic insight into the catalytic inhibition by nitroxides of tyrosine oxidation and nitration

Eric Maimon, Amram Samuni, Sara Goldstein

PII: S0304-4165(19)30189-8
DOI: https://doi.org/10.1016/j.bbagen.2019.07.012
Reference: BBAGEN 29403

To appear in: *BBA - General Subjects*

Received date: 23 May 2019
Revised date: 3 July 2019
Accepted date: 24 July 2019

Please cite this article as: E. Maimon, A. Samuni and S. Goldstein, Mechanistic insight into the catalytic inhibition by nitroxides of tyrosine oxidation and nitration, BBA - General Subjects, https://doi.org/10.1016/j.bbagen.2019.07.012

Mechanistic Insight into the Catalytic Inhibition by Nitroxides of Tyrosine Oxidation and Nitration

Eric Maimon[a], Amram Samuni[b], Sara Goldstein[c,*] sara.goldstein1@mail.huji.ac.il

[a]Nuclear Research Centre Negev and Chemistry Department, Ben-Gurion University, Beer-Sheva 84105, Israel

[b]Institute of Medical Research, Israel-Canada Medical School , The Hebrew University of Jerusalem, Jerusalem 91120, Israel

[c]Institute of Chemistry, The Accelerator Laboratory, the Hebrew University of Jerusalem, Jerusalem 91904, Israel

[*]Corresponding author.

Abstract

Background: Nitroxide antioxidants ($RNO^{\bullet}$) protect from injuries associated with oxidative stress. Tyrosine residues in proteins are major targets for oxidizing species giving rise to irreversible cross-linking and protein nitration, but the mechanisms underlying the protective activity of $RNO^{\bullet}$ on these processes are not sufficiently clear.

Methods: Tyrosine oxidation by the oxoammonium cation ($RN^{+}=O$) was studied by following the kinetics of $RNO^{\bullet}$ formation using EPR spectroscopy. Tyrosine oxidation and nitration were investigated using the peroxidase/H_2O_2 system without and with nitrite. The inhibitory effect of $RNO^{\bullet}$ on these processes was studied by following the kinetics of the evolved O_2 and accumulation of tyrosine oxidation and nitration products.

Results: Tyrosine ion is readily oxidized by $RN^{+}=O$, and the equilibrium constant of this reaction depends on $RNO^{\bullet}$ structure and reduction potential. $RNO^{\bullet}$ catalytically inhibits tyrosine oxidation and nitration since it scavenges both tyrosyl and $^{\bullet}NO_2$ radicals while recycling through $RN^{+}=O$ reduction by H_2O_2, tyrosine and nitrite. The inhibitory effect of nitroxide on tyrosine oxidation and nitration increases as its reduction potential decreases where the 6-membered ring nitroxides are better catalysts than the 5-membered ones.

Conclusions: Nitroxides catalytically inhibit tyrosine oxidation and nitration. The proposed reaction mechanism adequately fits the results explaining the dependence of the nitroxide inhibitory effect on its reduction potential and on the concentrations of the reducing species present in the system.

General Significance: Nitroxides protect against both oxidative and nitrative damage. The proposed reaction mechanism further emphasizes the role of the reducing environment to the efficacy of these catalysts.

Keywords: peroxidase, TPO, 3-CP, nitrotyrosine, dityrosine, ala-tyr, kinetics, mechanism, EPR

Abbreviations

$ABTS^{2-}$	2,2'-Azino-bis(3-ethylbenzthiazoline-6-sulfonic acid
$R\text{-}^{+\bullet}PorFe^{IV}=O$	compound I
$R\text{-}PorFe^{IV}=O$	compound II
3-CP	3-carbamoyl proxyl
	diethylenetriaminepentaacetic acid
DTPA	compound I and II of HRP, HRP-I and HRP-II
EPR	electron paramagnetic resonance
HRP	horseradish peroxidase
I	ionic strength
MPO	myeloperoxidase,
3-NT	3-nitrotyrosine
$R\text{-}PorFe^{III}$	peroxidase
PB	phosphate buffer
TCPO	2,2,5,5-tetramethyl-3-carbamido-3-pyrroline-1-oxyl
TPO	2,2,6,6-tetramethyl-piperidine-N-oxyl

1. Introduction

Stable cyclic nitroxide radicals ($RNO^{\bullet}$) have been long known to protect laboratory animals from injuries associated with a variety of oxidative stress conditions [1-5]. Yet, less attention has been directed at their inhibitory effect against nitration and specifically protein nitration. The chemistry of nitroxides is associated with a one-electron exchange among their reduced and oxidized states as demonstrated for 2,2,6,6-tetramethyl-piperidine-N-oxyl (TPO) in Scheme 1.

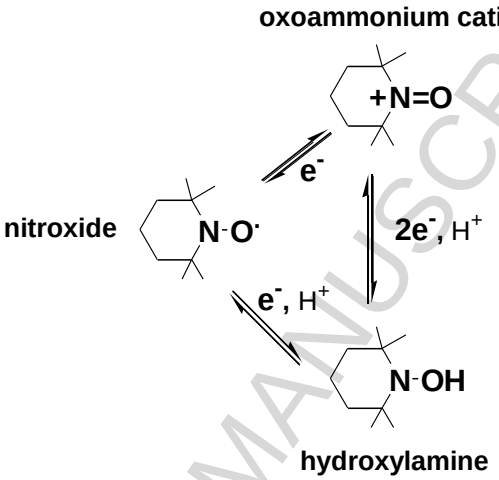

Scheme 1. Three oxidation states of 2,2,6,6-tetramethyl-piperidine-N-oxyl (TPO).

Nitroxides efficiently scavenge radicals yielding the respective oxoammonium cations ($RN^{+}=O$) through the formation of radical-radical intermediate adducts [6-9]. In the case of carbon-centered radicals the adducts are relatively stable [10,11] whereas in the case of thiyl radicals they decompose to yield the respective amines [12]. Moreover, nitroxides react with diverse biological oxidizing and reducing agents while being recycled through $RN^{+}=O$ reduction and hydroxylamine oxidation.

Tyrosine residues in proteins are major targets for oxidizing species yielding the respective tyrosyl radicals ($TyrO^{\bullet}$), which dimerize yielding dityrosine (a C-C linked dimer) and iso-diyrosine (a C-O linked dimer), and consequently give rise to irreversible cross-linking [13,14]. $TyrO^{\bullet}$ also adds to $^{\bullet}NO_2$ leading to protein nitration, which takes place under various disease conditions [15,16]. It has been demonstrated that nitroxides are efficient near-stoichiometric scavengers of

protein radicals [17]. The rate constant of TPO reaction with tyrosyl-derived radical has been determined to be $\approx 1 \times 10^8$ $M^{-1}s^{-1}$ demonstrating that TPO decreased the yields of tyrosine oxidation products in photo-oxidized cells [18]. It has also been shown that TPO and 4-OH-TPO inhibit tyrosine nitration induced by peroxidase/H_2O_2/nitrite, which has been attributed to an efficient scavenging of $^{\bullet}NO_2$ while ignoring that of $TyrO^{\bullet}$ [19-21]. In all previous studies the recycling of the nitroxides has been assumed to take place through the reduction of $RN^{+}=O$ by H_2O_2 overlooking its reduction by tyrosine and nitrite [19-21], which can compete with H_2O_2 for $RN^{+}=O$ leading to the formation of tyrosine oxidation and nitration products. Previously, we have shown that $RN^{+}=O$ is oxidized by $^{\bullet}NO_2$ and studied the kinetics of this reaction [8,22]. Here we have studied the kinetics of tyrosine oxidation by $RN^{+}=O$ as well as the inhibitory effect of nitroxides on tyrosine oxidation and nitration mediated by peroxidase/H_2O_2. The proposed reaction mechanism explains the dependence of the inhibitory effect of nitroxides on their reduction potential as well as on the concentrations of the reducing species present in the system.

2. Material and methods

2.1. Materials

Water for preparation of the solutions was purified using a Milli-Q purification system. All chemicals were of analytical grade and were used as received. The following products were purchased from Sigma-Aldrich: horseradish peroxidase (HRP, Type VI, A_{403}/A_{280}= 2.8 - 3.0), myeloperoxidase from human leukocytes (MPO, ≥50 units/mg protein, A_{430}/A_{280}= 0.74), 2,2'-Azino-bis(3-ethylbenzthiazoline-6-sulfonic acid ($ABTS^{2-}$), guaiacol, diethylenetriaminepentaacetic acid (DTPA), L-tyrosine, 3-nitro-L-tyrosine (3-NT), ala-tyr and gly-tyr. The nitroxides 2,2,6,6-tetramethyl-piperidine-1-oxyl (TPO), 4-OH-TPO, 4-amino-TPO, 4-carboxy-TPO, 3-carbamoylproxyl (3-CP), 3-carboxy-proxyl and 2,2,5,5-tetramethyl-3-carbamido-3-pyrroline-1-oxyl (TCPO) were purchased from Sigma-Aldrich and 4-oxo-TPO from Alexis Biochemicals. Scheme 2 displays the structures of the nitroxide derivatives studied.

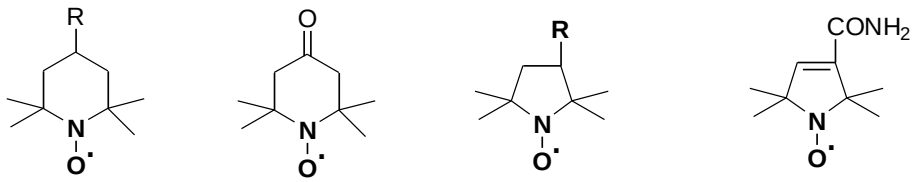

R = H (**TPO**)
R = OH
R = NH_2
R = COOH

4-oxo-TPO

R = $CONH_2$ (3-CP)
R = COOH

TCPO

Scheme 2. Structure of the nitroxide derivatives studied.

The oxoammonium cation of TPO and 3-CP were prepared electrochemically using the EmStat-PalmSens USB powered potentiostat electrochemical interface. Home-made electro-chemical cell consisted of a working electrode of graphite grains packed inside a porous Vycor glass tube (5 mm I.D.), through which the solution (100 - 200 μM $RNO^{\bullet}$, 10 mM $NaClO_4$) was pumped (165 μL s^{-1}). An outer glass cylinder, with separate electrolyte (10 mM phosphate buffer (PB), pH 7.0) contained the platinum auxiliary electrode and Ag/AgCl (in 3.5 M KCl) as a reference electrode. $RN^{+}=O$ readily oxidizes $ABTS^{2-}$, and the yield of $ABTS^{\bullet-}$ (ε_{660} = 12 $mM^{-1}cm^{-1}$) was used to determine $[RN^{+}=O]$ resulting in an oxidation yield between 80 - 90%. The residual $RNO^{\bullet}$ was determined by EPR spectroscopy demonstrating that $[RNO^{\bullet}]_0 \approx [RN^{+}=O] + [RNO^{\bullet}]$. H_2O_2 concentration was determined by the iodometric assay using ε_{352} = 25.8 $mM^{-1}cm^{-1}$ [23].

2.2. Peroxidase activity

HRP and MPO were dissolved in 10 mM PB, pH 6.3, and their concentration was determined spectrophotometrically using ε_{403} = 100 $mM^{-1}cm^{-1}$ [24] and ε_{430} = 91 $mM^{-1}cm^{-1}$ [25], respectively. HRP activity was determined using $ABTS^{2-}$ as a reducing substrate. An aliquot of 10 μL of enzyme solution was plunged into a cuvette containing 3 mL of 2 mM $ABTS^{2-}$, 1 mM H_2O_2 and 40 mM PB, pH 6.0. Oxidation of $ABTS^{2-}$ was monitored at 660 nm (ε_{660} = 12 $mM^{-1}cm^{-1}$), and the initial reaction rate was calculated over the first 60 s. MPO activity was determined using guaiacol as a reducing substrate [26]. An aliquot of 10 or 20 μL of enzyme solution was plunged into a cuvette

containing 3 mL of 50 mM guaiacol, 0.5 mM H_2O_2 and 40 mM PB at pH 7.0. Oxidation of guaiacol was monitored at 470 nm (ε_{470} = 26.6 $mM^{-1}cm^{-1}$), and the initial reaction rate was calculated over the first 60 s.

2.3. Tyrosine oxidation mediated by peroxidase/H_2O_2

Tyrosine oxidation catalyzed by peroxidase/H_2O_2 at pH 7.45 (40 mM PB) was monitored spectrophotometrically (HP 8452A diode array spectrophotometer) and fluorometrically (Perkin-Elmer LS-5) with excitation at 320 nm and emission at 412 nm after 1:20 dilution with 100 mM PB, pH 8.0 [27-30]. Tyrosine oxidation yields dimers, trimers and other polymers of tyrosine, which are fluorescent and absorb similarly at the UV region, although having different quantum yields and molar extinction coefficients, respectively [30-34]. Therefore, calibration curves were not preformed, and the measured absorption and fluorescence are attributed to all tyrosyl addition products. The experiments have been carried out using solutions of 40 mM PB, pH 7.45 containing 50 μM DTPA at room temperature. The reaction was followed where tyrosine oxidation products absorb (315 nm [30-34]) and the contribution of tyrosine and peroxidase absorption is minimal. The reported ΔA_{315} and the initial rate are from at least three separate experiments.

2.4. Tyrosine nitration mediated by HRP/H_2O_2/nitrite

Peroxidases catalyze tyrosine nitration and oxidation by H_2O_2 and nitrite. As the pH increases, the yield of tyrosine oxidation products increases at the expense of the nitration products, *i.e.*, 3-NT (pK_a = 7.35 [35]), because in this system the rate of tyrosine oxidation is pH-independent while that of nitrite oxidation decreases as the pH increases [21,36]. The protonated form of 3-NT absorbs at 356 nm whereas the deprotonated form absorbs at 430 nm. Using commercial 3-NT, we determined $\varepsilon_{357} = 2630 \pm 50$ $M^{-1}cm^{-1}$ in 40 mM PB at pH 6.0 and $\varepsilon_{430} = 4180 \pm 100$ $M^{-1}cm^{-1}$ at pH >10, which is in agreement with an earlier reported value of 4200 $M^{-1}s^{-1}$ [35]. The literature value at acidic solution, *i.e.*, ε_{350} = 3400 $M^{-1}s^{-1}$ [35], is too high most probably due to the absorption of residual tyrosine. The experiments were carried out using solutions of 40 mM PB at pH 6 containing 50 μM DTPA at room temperature where the yield of tyrosine oxidation products having maximum

absorption around 290 nm [30-34] is relatively low. The kinetics of 3-NT formation was monitored at 356 nm and its yield was also verified by its absorption at 430 nm upon alkalization. The reported yields of 3-NT are from at least three separate experiments.

2.5. Oximetry

O_2 evolution was monitored using a Clark electrode coupled to an YSI Model 5300 Biological Oxygen Monitor unit, interfaced with a PC computer. The sample was continuously stirred during the experiments and the temperature of the oximeter cell (1.62 mL volume) was controlled at 25 ± 0.2°C using a Julabo F10 circulating water bath. Argon was bubbled through the solution for experiments requiring anoxic conditions. After temperature equilibration, the reaction was started by injecting up the peroxidase through the stopper of the oximeter cell. Each experiment was calibrated using aerated and anoxic samples, and was further confirmed by measuring O_2 yield produced upon the injection of catalase through the stopper of the cell into standard H_2O_2 solution.

2.6. Electron paramagnetic resonance (EPR)

EPR spectra were recorded using a Varian E4 X-band spectrometer operating at 9.36 GHz with the center field set at 3325 G, 100 kHz modulation frequency, 2 G field modulation amplitude, and 20 mW incident microwave power at room temperature. Samples of the reaction mixture were injected into a flexible capillary, which was inserted into a quartz tube placed within the EPR spectrometer cavity. $RNO^{\bullet}$ concentration was calculated from the EPR signal intensity of standard solutions of $RNO^{\bullet}$.

2.7. Kinetic simulation

Modeling of the experimental results was carried out using INTKIN, a non commercial program developed at Brookhaven National Laboratories by Dr. H. A. Schwarz.

3. Results

3.1. Tyrosine oxidation by $RN^+=O$

Using pulse radiolysis, the rate constant of TPO reaction with N-acetyl-L-tyrosinamide-derived $TyrO^\bullet$ has been determined to be $k_1 = (1.47 \pm 0.12) \times 10^8\ M^{-1}s^{-1}$ overlooking the back reaction -1 [18].

$$RNO^\bullet + TyrO^\bullet \rightleftharpoons RN^+=O + TyrO^- \quad (1)$$

$$2\ TyrO^\bullet \rightarrow \text{dityrosine} \qquad 2k_2 = 4.5\times10^8\ M^{-1}s^{-1}\ [37] \quad (2)$$

The back reaction -1 cannot be ignored since $E^0(TPO^+/TPO) = 0.74$ V [8] and $E^0(TyrO^\bullet/TyrO^-) = 0.72$ V [38], which is close to that of tyrosyl residue in peptides [39]; that is $K_1 \approx 0.5$. In addition, $TyrO^\bullet$ was generated *via* tyrosine (2.2 – 2.5 mM) oxidation by azide radical in the presence of 25 – 125 μM TPO at pH 7.4, and under these experimental conditions a mixture of $TyrO^\bullet$ and TPO^+ is initially formed *via* the oxidation of both tyrosine and TPO by azide radicals [18]. Indeed, the kinetic traces of $TyrO^\bullet$ absorption decay in the presence of TPO show that $TyrO^\bullet$ does not decay to zero, and that the residual absorption depends on $[TPO]_0$ [18].

The contribution of reaction -1 is demonstrated by studying directly the reaction of tyrosine with $RN^+=O$ (reactions -1). Assuming a fast approach to equilibrium 1, the rate-determining step for the decay of $RN^+=O$ in the presence of an excess of tyrosine is the dimerization of $TyrO^\bullet$ whose concentration is determined by equilibrium 1. Hence, rate equation 3 is obtained where $a = [RN^+=O]_t + [RNO^\bullet]_t$, $[RN^+=O]_t = x$ and $pK_a = 10.3$ at low ionic strength ($I = 0.04$ M) [40].

$$-\frac{dx}{dt} = 2k_2[TyrO^\bullet]_t^2 = \frac{2k_2K_a^2[TyrOH]_0^2[RN^+=O]_t^2}{K_1^2[H^+]^2[RNO^\bullet]_t^2} = \frac{kx^2}{(a-x)^2} \quad (3)$$

The differential equation 3 is easily solved having logarithmic, inverse, and linear terms:

$$2a\ln\left(\frac{x}{a}\right) + \frac{a^2}{x} - x = kt \qquad (4)$$

The reaction of excess of tyrosine with TPO^+ and 3-CP^+ at different pHs was studied by following the formation of the nitroxide by EPR spectroscopy. $RN^+=O$ was fully reduced to $RNO^\bullet$, and in the case of TPO^+ and TyrOH, the formation of TPO obeyed second-order kinetics implying that the logarithmic and linear terms in eq. 4 are negligible (Fig. 1).

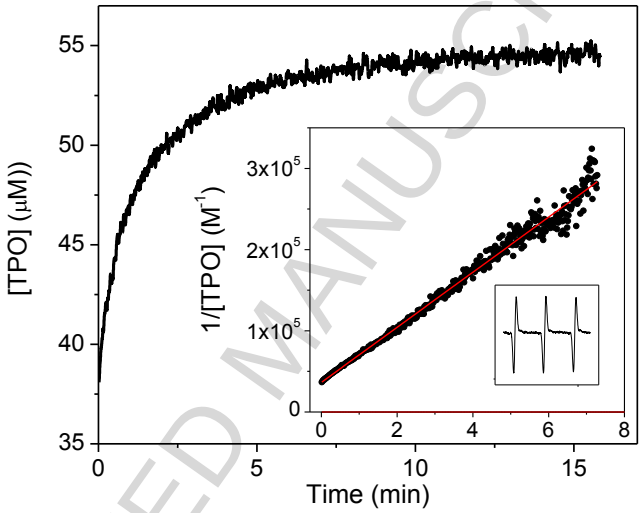

Figure 1. **TyrOH oxidation by TPO^+**. Kinetics of TPO formation *via* TPO^+ (50 μM contaminated with 7 μM TPO) reaction with TyrOH (660 μM) at pH 6.2 (24 mM PB). The inset contains a fit to a second-order reaction and the final EPR spectrum of 55 μM TPO. The reaction was followed by monitoring the intensity of the middle EPR line. Field 3324 G, Power 20W, Mod 2G, TC 0.064 s.

Equation 5 is obtained for $1/\tau_{1/2}$ where $x = a/2$:

$$\frac{1}{\tau_{1/2}} = \frac{k}{0.114a} = \frac{2k_2K_a^2[\mathrm{TyrOH}]_0^2}{0.114[\mathrm{RN^+{=}O}]_0K_1^2[\mathrm{H^+}]^2} \qquad (5)$$

A plot of $1/\tau_{1/2}$ *vs.* $[\text{ala-tyr}]_0^2$ at constant pH is linear as demonstrated for TPO^+ reaction with ala-tyr (Fig. 2A) whose solubility in water is higher than that of TyrOH. From the slope of the line in Fig.

2A one calculates $K_1 \approx 1.4$ resulting in E^0(ala-tyrO$^\bullet$/ala-tyrO$^-$) ≈ 0.75V, which is similar to the reported reduction potential of ala-tyr-ala and gly-tyr, *i.e.*, 0.74 and 0.75 V, respectively [39].

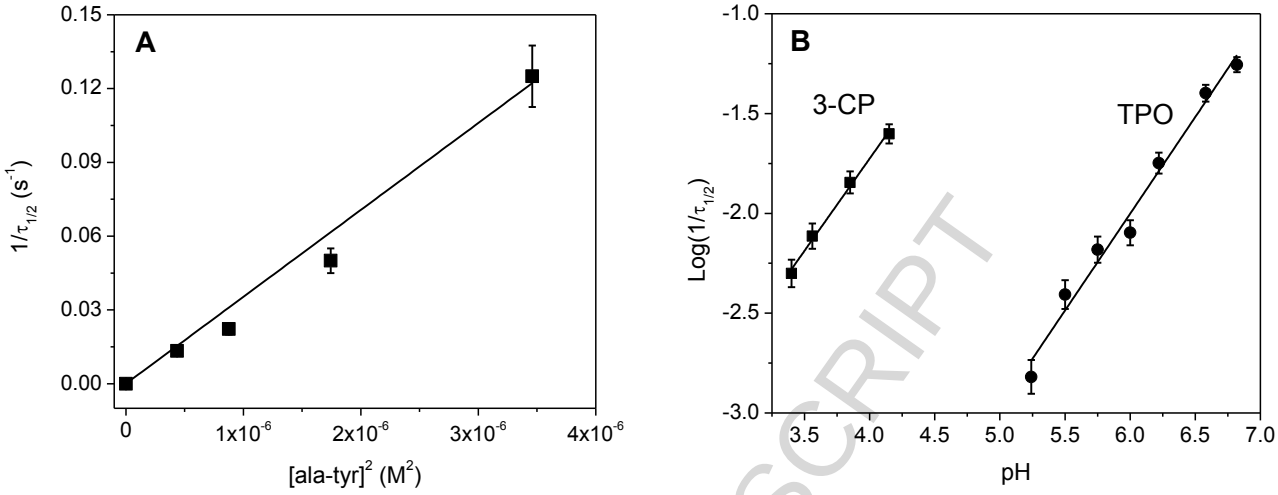

Figure 2. Half-life of tyrosine oxidation by RN$^+$=O. (A) Dependence of $1/\tau_{1/2}$ on [ala-tyr]^2 (50 µM TPO$^+$, pH 5.75, 24 mM PB); (B) pH-dependence of $\log(1/\tau_{1/2})$ of the formation of RNO$^\bullet$ upon TyrOH (660 µM) reaction with RN$^+$=O (50 µM). Field 3324 G, Power 20W, Mod 2G, TC 0.064 s. RN$^+$=O solutions were contaminated with less than 15% RNO$^\bullet$.

According to eq. 5, a plot of $\log(1/\tau_{1/2})$ *vs.* pH is linear as demonstrated for TPO$^+$ and 3-CP$^+$ displaying slopes of 0.97 ± 0.06 and 0.92 ± 0.05, respectively (Fig. 2B). Using E^0(TyrO$^\bullet$/TyrO$^-$) = 0.72 V [38] and E^0(RN$^+$=O/RNO$^\bullet$) = 0.74 and 0.87 V for TPO and 3-CP, respectively [8], one calculates $K_1 = 0.46$ for TPO and 2.9×10^{-3} for 3-CP. Thus, K_1 can be calculated for any RNO$^\bullet$ and tyrosine where only k_1 is pH-independent. In the case of TPO, k_1 has been determined to be $\approx 10^8$ M^{-1}s^{-1} at pH 7.4 [18], *i.e.*, $k_{-1} \approx 2 \times 10^8$ M^{-1}s^{-1}. If the same k_1-value applies for 3-CP, the calculated $k_{-1} \approx 3.5 \times 10^{10}$ M^{-1}s^{-1} is unreasonably high. Previously, a difference of about 2 orders of magnitude has been found between the rate constants of TPO and 3-CP reactions with $HO_2^\bullet$ [41] and $RO_2^\bullet$ [9], and this is most probably the case also with TyrO$^\bullet$, *i.e.*, $k_1 \approx 10^6$ M^{-1}s^{-1} for 3-CP.

3.2. $RNO^{\bullet}$ inhibits tyrosine oxidation mediated by peroxidase/H_2O_2

Peroxidase (R-PorFe^{III}) catalyzes tyrosine oxidation by H_2O_2 *via* reactions 6 – 8 where reaction 8 is the rate-determining step [33,34,42].

$$\text{R-PorFe}^{III} + H_2O_2 \rightarrow \text{R-}^{+\bullet}\text{PorFe}^{IV}\text{=O} + H_2O \quad (6)$$

$$\text{R-}^{+\bullet}\text{PorFe}^{IV}\text{=O} + \text{TyrO}^{-} \rightarrow \text{R-PorFe}^{IV}\text{=O} + \text{TyrO}^{\bullet} \quad (7)$$

$$\text{R-PorFe}^{IV}\text{=O} + \text{TyrO}^{-} + 2H^{+} \rightarrow \text{R-PorFe}^{III} + \text{TyrO}^{\bullet} + H_2O \quad (8)$$

TyrOH oxidation initially produces dityrosine (reaction 2), but further oxidation also produces trityrosine, isodityrosine and pulcherosine [32-34].

The heme species of the enzyme observed upon the addition of H_2O_2 to HRP solutions containing excess of tyrosine over H_2O_2 without and with nitroxide is mainly R-PorFe^{IV}=O (compound II) because the rate-determining step is reaction 8. Tyrosine protects HRP against inactivation induced by H_2O_2 as previously reported [43]. Therefore, during the course of the catalysis there is no loss of compound II of HRP, and the spectrum of the native enzyme reappears upon complete consumption of H_2O_2. Unlike HRP, MPO (20-50 nM) was fully inactivated by H_2O_2 (115-380 μM) in the presence of 1 mM TyrOH, but the addition of TPO protected the enzyme, *e.g.*, 95 μM TPO provided 90% protection for 20 nM MPO in the presence of 380 μM H_2O_2.

Kinetic traces of TyrOH oxidation mediated by HRP/H_2O_2 in the presence of TPO are shown in Fig. 3A demonstrating unique shapes where the inhibition is substantial as will be explained below. TPO inhibits TyrOH oxidation in a dose dependent manner as reflected by the same effect on ΔA_{315} and on the fluorescence (*F)* (Fig. 3B). Where the inhibitory effect of the nitroxide is substantial, its effect on the initial rate of A_{315} formation (R_{315}) is higher compared to its effect on ΔA_{315} or *F*, *e.g.*, 40 μM TPO inhibits 84% of the yield but 92% of the initial rate (Fig. 3), as will be explained below.

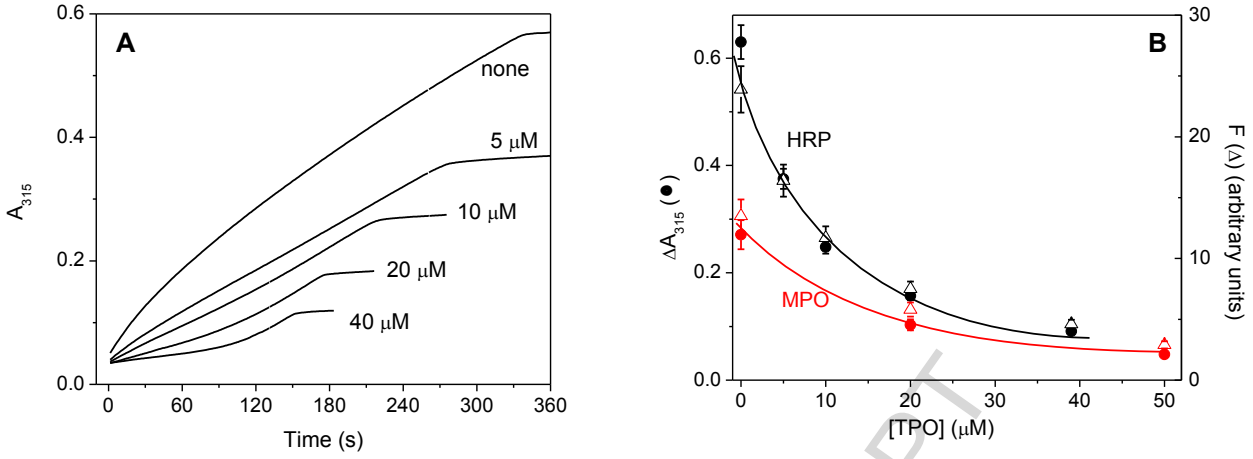

Figure 3. **TPO inhibits tyrosine oxidation induced by peroxidase/H_2O_2.** (A) Kinetic traces monitored at 315 nm of the accumulation of TyrOH oxidation products induced by1 μM HRP, 300 μM H_2O_2, and 1 mM TyrOH in the absence and presence of 5, 10, 20, and 40 μM TPO; (B) Effect of [TPO] on ΔA_{315} and fluorescence (F) induced by 1 μM HRP, 300 μM H_2O_2 and 1 mM TyrOH and by 50 nM MPO, 115 μM H_2O_2 and 1 mM TyrOH. All solutions contained 50 μM DTPA and 40 mM PB at pH 7.45.

Tyrosine oxidation inhibited by $RNO^{\bullet}$ is attributed to its reaction with $TyrO^{\bullet}$ forming $RN^{+}=O$ (reaction 1), which is reduced back to $RNO^{\bullet}$ by HO_2^{-} (pK_a = 11.75) and by $O_2^{\bullet-}$ (pK_a = 4.8) *via* reactions 9 and 10, respectively [41].

$$RN^{+}=O + HO_2^{-} \rightleftharpoons RNO^{\bullet} + HO_2^{\bullet} \quad (9)$$

$$RN^{+}=O + O_2^{\bullet-} \rightarrow RNO^{\bullet} + O_2 \quad (10)$$

There is a competition between the reactions of H_2O_2 and tyrosine for $RN^{+}=O$. Therefore, as $[H_2O_2]$ progressively decreases, the contribution of $RN^{+}=O$ reduction by tyrosine (reaction -1) increases giving rise to dityrosine formation and to unusual kinetic profiles especially where the inhibitory effect is substantial, namely where R_{315} is relatively low (Fig. 1A). In addition, the inhibitory effect of $RNO^{\bullet}$ increases upon increasing $[tyrosine]_0$ as demonstrated in Table 1. The inhibitory effect of $RNO^{\bullet}$ on TyrOH oxidation is significantly greater compared to ala-tyr oxidation because the rate constants of reactions 7 and 8 in the case of ala-tyr are about an order of magnitude higher

compared to TyrOH (Fig. A.1, supplementary materials), and the steady-state concentration of $TyrO^{\bullet}$ in the case of ala-tyr is higher; that is $k_2[TyrO^{\bullet}]^2$ is higher.

Table 1. Inhibitory effect of 10 μM TPO on tyrosine oxidation *vs.* [tyrosine]$_0$. Initial oxidation rates (R_{315}) and yields (ΔA_{315} and F) induced by 0.5 μM HRP and 90 μM H_2O_2 at pH 7.45.

Substrate (mM)	$R_{315}/R_{315}(0)^a$	$\Delta A_{315}/\Delta A_{315}(0)^b$	$F/F(0)^b$
TyrOH (0.2)	0.10	0.18	0.26
TyrOH (0.4)	0.31	0.35	0.38
TyrOH (0.7)	0.53	0.55	0.56
TyrOH (1)	0.60	0.65	0.66
ala-tyr (0.4)	0.59	0.58	0.58
ala-tyr (1)	0.90	0.84	0.79

a – R_{315} and $R_{315}(0)$ are the initial oxidation rates with and without TPO, respectively; *b* – Oxidation yield expressed as $\Delta A_{315}/\Delta A_{315}(0)$ and $F/F(0)$ where $\Delta A_{315}(0)$ and $F(0)$ are in the absence of TPO. The experimental error is ±10%.

The comparison between the inhibitory effects of various nitroxides on TyrOH oxidation is shown in Table 2 demonstrating that the efficacy of the 6-membered ring nitroxides follows the order TPO > 4-NH_3^+-TPO > 4-OH-TPO ≈ 4-COO^--TPO > 4-oxo-TPO; that is the nitroxide inhibitory activity increases as its reduction potential decreases. The inhibitory effect of the positively charged nitroxide (4-NH_3^+-TPO, 0.82-0.85 V) is higher and that of the negatively charged one (4-COO^--TPO, 0.77 V) is lower compared to 4-OH-TPO (0.82 V) most probably due to ionic strength effect on k_{-1}-value, *i.e.*, k_{-1}-value for the +2 charged nitroxide is the lowest since $\log(k/k_0) = 1.02 Z_A Z_B I^{1/2}$ where k_0 is at $I = 0$, $Z_A = -1$ for $TyrO^-$ and $Z_B = 0$, +1 and +2 for 4-COO^--TPO^+, 4-OH-TPO^+ and 4-NH_3^+-TPO^+, respectively. The 5-membered ring nitroxides are less effective catalysts than the 6-membered ones because their respective k_1-values are about two orders of magnitude lower. Their inhibitory effect also decreases as the reduction potential increases following the order 3-COO^--proxyl > 3-CP > TCPO. In this case the difference in the reduction potential between 3-COO^--proxyl and 3-CP is relatively high and overcomes the ionic strength effect.

Table 2. Effect of $RNO^{\bullet}$ structure on the initial oxidation rate (R_{315}) mediated by 1 μM HRP and 0.3 mM H_2O_2 in the presence of 1 mM TyrOH at pH 7.45.[a]

$RNO^{\bullet}$	$E^0(RN^+{=}O/RNO^{\bullet})$, mV[a]	$[RNO^{\bullet}]$, μM	$R_{315}/R_{315}(0)$[b]
TPO	0.74	20	0.20
4-NH_3^+-TPO[c]	0.82-85	20	0.40
4-OH-TPO	0.82	20	0.67
4-COO^--TPO[d]	0.77	20	0.65
4-COO^--TPO		100	0.12
4-oxo-TPO	0.92	100	0.77
4-oxo-TPO		300	0.55
3- COO^--proxyl[e]	0.79	100	0.58
3- COO^--proxyl		300	0.26
3-CP	0.87	300	0.83
3-CP		500	0.66
TCPO	0.96	500	0.92

a – Taken from ref. [8].
b – R_{315} and $R_{315}(0)$ are the initial rates with and without $RNO^{\bullet}$, respectively. The experimental error is ±10%.
c – pK_a = 9.1; *d* – pK_a = 4.0; *e* – pK_a = 3.4 (taken from ref. [8]).

In the HRP/H_2O_2/tyrosine system H_2O_2 is reduced to H_2O, but in aerated solutions some consumption of O_2 takes place most probably due to O_2 reaction with tyrosyl radicals, which has been reported to be slow, *i.e.*, $k < 1 \times 10^3$ $M^{-1}s^{-1}$ [44]. For example, under aerated conditions about 27 μM O_2 is consumed during the oxidation of 1 mM TyrOH by 0.5 mM H_2O_2 catalyzed by 2 μM HRP. However, in the presence of any nitroxide, the kinetics and extent of the evolved O_2 are essentially the same in anoxic and aerated solutions implying that the contribution of tyrosyl reaction with O_2 is insignificant. In the presence of $RNO^{\bullet}$ the inhibition of tyrosine oxidation is accompanied by O_2 released since $RNO^{\bullet}$ is recycled *via* reactions 9 and 10. The extent of O_2 released depends on $RNO^{\bullet}$ structure and increases as its concentration increases approaching $[H_2O_2]_o/2$ (Fig. 4), *i.e.*, $RNO^{\bullet}$ converts the peroxidative activity into catalatic one.

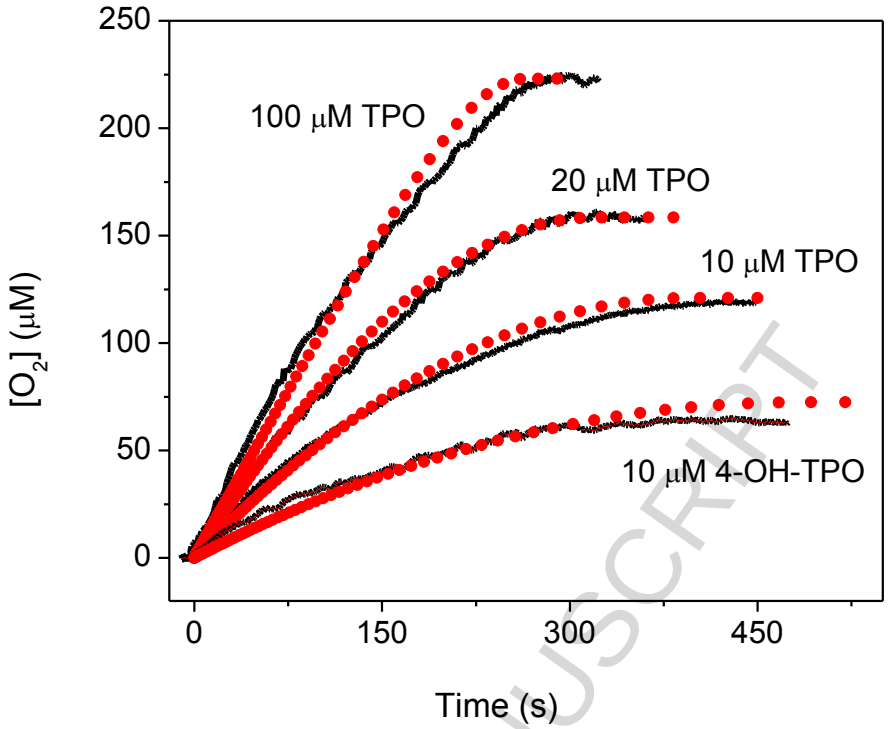

Figure 4. O_2 released induced by HRP/H_2O_2 in the presence of RNO$^\bullet$. Kinetics of O_2 released induced by 1 μM HRP, 0.5 mM H_2O_2, 1 mM TyrOH and RNO$^\bullet$ as indicated in the figure. Anoxic solutions contained 50 μM DTPA and 40 mM PB at pH 7.45. The red dotted curves represent simulated data using the proposed mechanism (Scheme 3) and the rate constants listed in Table 4 where k_{-1}(app) = 2.8 x 10^5 $M^{-1}s^{-1}$ (TPO) and 1.04 x 10^7 $M^{-1}s^{-1}$ (4-OH-TPO).

The nitroxides tested differ by their effect on the extent of O_2 released, which reflects their inhibitory effect on tyrosine oxidation yield, following the order TPO > 4-OH-TPO > 4-oxo-TPO > 3-CP.

The EPR signal intensity of RNO$^\bullet$ was measured before the addition of H_2O_2 and upon its complete consumption. No loss of the EPR signal intensity was detected implying that all nitroxides act catalytically.

3.3. RNO$^\bullet$ inhibits tyrosine nitration mediated by HRP/H_2O_2/nitrite

When nitrite is included in the HRP/H_2O_2/tyrosine mixture, it competes with tyrosine for compounds I and II forming $^\bullet NO_2$, which readily adds to TyrO$^\bullet$ (k_{13} = 3 x 10^9 $M^{-1}s^{-1}$ [45]) and oxidizes tyrosine ion (k_{14} = 2.9 x 10^7 $M^{-1}s^{-1}$, pH 12 [46]).

$$R\text{-}^{+\bullet}PorFe^{IV}{=}O + NO_2^- \rightarrow R\text{-}PorFe^{IV}{=}O + {}^{\bullet}NO_2 \quad (11)$$

$$R\text{-}PorFe^{IV}{=}O + NO_2^- + 2H^+ \rightarrow R\text{-}PorFe^{III} + {}^{\bullet}NO_2 + H_2O \quad (12)$$

$$TyrO^{\bullet} + {}^{\bullet}NO_2 \rightarrow \text{adduct} \rightarrow \text{3-NT (45±5\% yield [47])} + \text{products} \quad (13)$$

$$TyrO^- + {}^{\bullet}NO_2 \rightleftharpoons TyrO^{\bullet} + NO_2^- \quad (14)$$

Previously, we have shown that TPO and 4-OH-TPO at μM concentrations inhibit, in a dose dependent manner, TyrOH nitration induced by peroxidase/H_2O_2/nitrite [21]. The inhibitory effect by these nitroxides was similar, and we have suggested that $RNO^{\bullet}$ efficiently competes with $TyrO^{\bullet}$ for ${}^{\bullet}NO_2$ (reactions 15) overlooking reactions 1, -1 and -15 [21].

$$RNO^{\bullet} + {}^{\bullet}NO_2 \rightleftharpoons RN^+{=}O + NO_2^- \quad (15)$$

Under this assumption the inhibitory effect on tyrosine nitration by all nitroxides should be the same since $k_{15} = (5 - 7) \times 10^8\ M^{-1}s^{-1}$ is independent of nitroxide reduction potential and structure [8]. Here we extend this study to other nitroxides investigating also the kinetics of 3-NT formation and O_2 released. Typical kinetic traces of 3-NT formation in the absence and presence of various nitroxides are shown in Fig. 5 demonstrating the same unusual shapes observed for tyrosine oxidation (Fig. 3A).

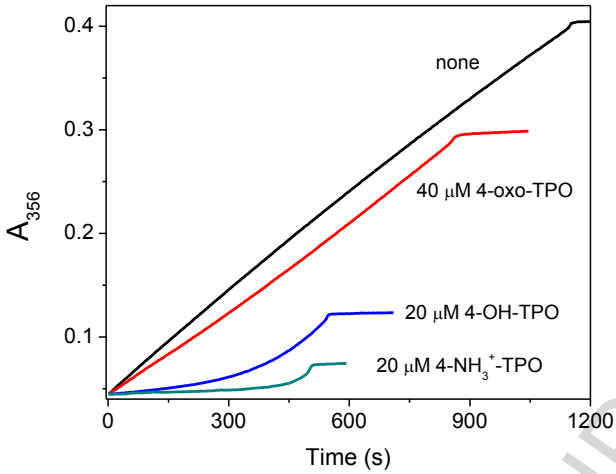

Figure 5. Kinetic traces of 3-NT formation (monitored at 356 nm) mediated by 0.5 μM HRP, 0.3 mM H_2O_2, 0.44 mM TyrOH, 1 mM nitrite in the absence and presence of $RNO^{\bullet}$ at pH 6.0.

The results summarized in Fig. 6 show that the effect of the nitroxides on the initial rate of 3-NT formation is dose dependent following the order 4-NH_3^+-TPO > TPO ≈ 4-OH-TPO >> 4-oxo-TPO > 3-CP.

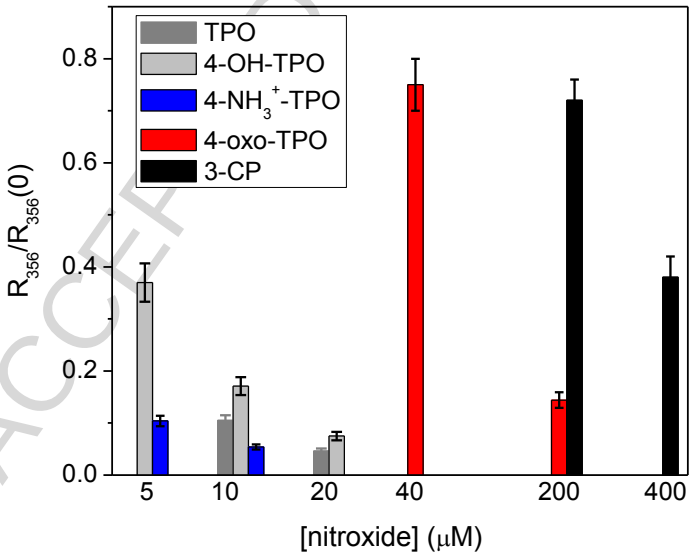

Figure 6. Effect of [$RNO^{\bullet}$] on the initial rate of TyrOH nitration (R_{356}) mediated by 0.5 μM HRP, 0.3 mM H_2O_2, 0.44 mM TyrOH and 1 mM nitrite in aerated solutions containing 40 mM PB and 50 μM DTPA, pH 6.0.

The kinetic traces in Fig. 5 demonstrate that the effect of the nitroxide on 3-NT rate and yield is substantial while the nitroxide is recycled *via* reactions 9 and 10. However, as $[H_2O_2]$ progressively decreases the yield of 3-NT increases because tyrosine and nitrite compete with H_2O_2 for $RN^+=O$ (reactions -1, -15). Due to this competition, the inhibitory effect of $RNO^\bullet$ on tyrosine nitration decreases as $[TyrOH]_0$ and $[nitrite]_0$ increase (Table 3).

Table 3. Inhibitory effect of nitroxides decreases as $[TyrOH]_0$ and $[nitrite]_0$ increase. Initial rate of 3-NT formation (R_{356}) mediated by 0.5 μM HRP and 0.3 mM H_2O_2 at pH 6.0.

$RNO^\bullet$	$[RNO^\bullet]$, μM	$R_{356}/R_{356}(0)$ at 1 mM TyrOH 2 mM nitrite	$R_{356}/R_{356}(0)$ at 0.44 mM TyrOH 1 mM nitrite
4-OH-TPO	10	0.72	0.17
	20	0.37	0.075
4-NH_3^+-TPO	5	0.32	0.10
	10	0.18	0.053

R_{315} and $R_{315}(0)$ are the initial rates with and without $RNO^\bullet$, respectively. The experimental error is ±10%.

The formation of 3-NT ceased when H_2O_2 is fully consumed and HRP reappears. During this process O_2 is released (reactions 9 and 10), and the extent of O_2 released increases upon increasing $[RNO^\bullet]$ as demonstrated for 4-OH-TPO in Fig. 7A. The extent of O_2 released follows the order 4-NH_3^+-TPO > 4-OH-TPO > 4-oxo-TPO > 3-CP (Fig. 7), which is the same order as their inhibitory effect on 3-NT formation.

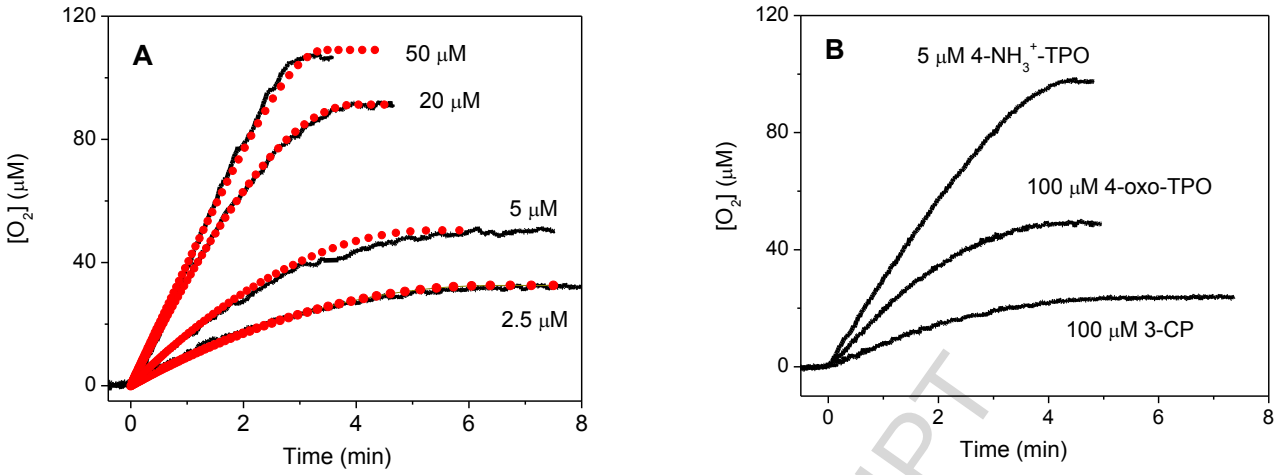

Figure 7. O_2 released by 1 μM HRP, 0.25 mM H_2O_2, 0.44 mM TyrOH and 1 mM nitrite in the presence of $RNO^{\bullet}$ at pH 6.0. (A) 2.5, 5, 20 and 50 μM 4-OH-TPO ; (B) 5 μM 4-NH_3^+-TPO, 100 μM 4-oxo-TPO and 100 μM 3-CP. The red dotted curves represent simulated data using the proposed mechanism and the rate constants listed in Table 4 where k_{-1}(app) = (2.5 ± 0.5) x 10^5 $M^{-1}s^{-1}$ and k_9 = 2 x 10^4 $M^{-1}s^{-1}$.

The inhibitory effect of the nitroxides is catalytic since there is hardly any loss of their EPR signal intensity except for about 20% loss in the case of TPO and 4-oxo-TPO.

4. Reaction mechanism

The proposed mechanism for HRP-catalyzed tyrosine oxidation by H_2O_2 in the presence of $RNO^{\bullet}$ is given in Scheme 3, and the rate constants are listed in Table 4. Table 4 includes also the reactions of compounds I and II with dityrosine, which in the presence of $RNO^{\bullet}$ are insignificant due to the low production of dityrosine. Under our experimental conditions the contribution of $RNO^{\bullet}$ oxidation by compounds I and II is insignificant [48].

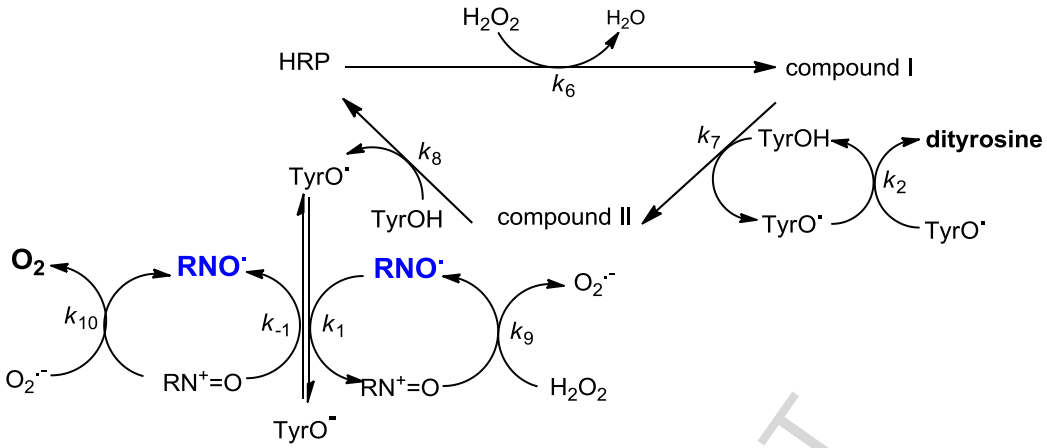

Scheme 3. Proposed mechanism for HRP-catalyzed tyrosine oxidation in the presence of RNO$^{\bullet}$

Since ΔA_{315} is due to all tyrosyl addition products, only modeling of the kinetics of O_2 released was performed where the extent of O_2 released reflects the inhibitory effect of RNO$^{\bullet}$ on tyrosine oxidation. The simulation adequately fits the experimental data shown in Fig. 4 using the literature values of all rate constants (Table 4). The simulated values of k_{-1}(app) at pH 7.45 are 2.8 x 10^5 and 1 x 10^7 $M^{-1}s^{-1}$ for TPO and 4-OH-TPO, respectively; that is K_1 = 0.5 and 0.014, respectively, which are in excellent agreement with those calculated using E^0(TyrO$^{\bullet}$/TyrO^{-}) = 0.72 V [38] and E^0(RN^{+}=O/RNO$^{\bullet}$) = 0.74 and 0.81 V for TPO and 4-OH-TPO, respectively. The proposed reaction mechanism demonstrates that the nitroxide inhibitory effect depends on the ratio k_{-1}(app)[tyrosine]/k_9(app)[H_2O_2] and explains the increase in the yield of tyrosine oxidation products as [H_2O_2] progressively decreases.

Table 4. Rate constants used for simulation of HRP-catalyzed tyrosine oxidation/nitration by H_2O_2 in the presence of TPO and 4-OH-TPO.

Reaction No.	k, K	*Ref.*
1[a]	$k_1 = 10^8$ $M^{-1}s^{-1}$ (TPO)	[18]
	$K_1 = 0.46$ (4-OH-TPO)	This study
	$K_1 = 0.02$ (4-OH-TPO)	This study
2	2.25×10^8 $M^{-1}s^{-1}$	[37]
6	1.7×10^7 $M^{-1}s^{-1}$	[49]
7	$(2.9 \pm 0.2) \times 10^4$ $M^{-1}s^{-1}$	This study
8	$(1.1 \pm 0.1) \times 10^3$ $M^{-1}s^{-1}$	This study
9 [b]	7×10^3 $M^{-1}s^{-1}$ (TPO, pH 7.45)	[41]
	250 $M^{-1}s^{-1}$ (TPO, pH 6.0)	
	1.1×10^5 $M^{-1}s^{-1}$ (4-OH-TPO, pH 7.45)	
	3.9×10^3 $M^{-1}s^{-1}$ (4-OH-TPO, pH 6.0)	
10	3×10^9 $M^{-1}s^{-1}$	[41]
11	$(3.2 \pm 0.2) \times 10^3$ $M^{-1}s^{-1}$ (pH 6.0)	[21]
12	170 ± 10 $M^{-1}s^{-1}$ (pH 6.0)	[21]
13	3×10^9 $M^{-1}s^{-1}$ (45±5% yield of 3-NT)	[45,47]
14 [c]	2.9×10^7 $M^{-1}s^{-1}$ (pH 12), $K_{14} = 8.2 \times 10^4$	[46]
15 [d]	7×10^8 $M^{-1}s^{-1}$	[8,22]
	$K_{15} = 1.9 \times 10^4$ (TPO); 4.2×10^5 (4-OH-TPO)	
Com I + dityr	3×10^3 $M^{-1}s^{-1}$	[33]
Com II + dityr	200 $M^{-1}s^{-1}$	[33]

a – K_1 calculated using $E^0(TyrO^{\bullet}/TyrO^-) = 0.72$ V, $E^0(RN^+{=}O/RNO^{\bullet}) = 0.74$ and 0.82V for TPO and 4-OH-TPO, respectively.
b – K_9 calculated using $E^0(HO_2^{\bullet}/HO_2^-) = 0.75$ V, $E^0(RN^+{=}O/RNO^{\bullet}) = 0.74$ and 0.82V for TPO and 4-OH-TPO, respectively, and k_9(app) was calculated using $k_{-9} = (1.4{\pm}0.1) \times 10^8$ $M^{-1}s^{-1}$ for both nitroxides [8].
c – K_{14} calculated using $E^0(TyrO^{\bullet}/TyrO^-) = 0.72$ V and $E^0(NO_2^{\bullet}/NO_2^-) = 1.01$ V.
d – K_{15} calculated using $E^0(NO_2^{\bullet}/NO_2^-) = 1.01$ V and $E^0(RN^+{=}O/RNO^{\bullet}) = 0.74$ and 0.82V for TPO and 4-OH-TPO, respectively.

The proposed reaction mechanism in the presence of nitrite includes also reactions 11 – 15 and their rate constants are listed in Table 4. In this system both tyrosine nitration and oxidation take place, but we only monitored 3-NT formation and O_2 released. Modeling of O_2 released is more accurate than that of 3-NT accumulation at 356 nm since it is independent of the yield of 3-NT formed *via* reaction 13. In addition there are also other species absorbing at 356 nm, which might interfere. Modeling of O_2 released in the case of 4-OH-TPO using reactions 1, 2, 6 –15 and the rate constants listed in Table 4 (pH 6.0) fits the experimental results in Fig. 7A using k_{-1}(app) = $(2.5 \pm 0.5) \times 10^5$ $M^{-1}s^{-1}$ (*i.e.*, $K_1 = 0.02$) and $k_9 = 2 \times 10^4$ $M^{-1}s^{-1}$, which is ca. 5-fold higher than the calculated value. The latter value can be rationalized assuming that 4-OH-TPO^+ reacts also with H_2O_2 with a rate constant, which is about 5-orders of magnitude lower than that with HO_2^-, $k_9 = 2.2 \times 10^9$ $M^{-1}s^{-1}$.

5. Conclusions

Nitroxides catalytically inhibit tyrosine oxidation and nitration. The proposed reaction mechanism explains the dependence of the nitroxide inhibitory effects on its structure and reduction potential. The rate constant of $RNO^{\bullet}$ reaction with $^{\bullet}NO_2$ is $(5 - 7) \times 10^8$ $M^{-1}s^{-1}$ independent of the nitroxide structure and reduction potential while that with $TyrO^{\bullet}$ is $\approx 10^8$ $M^{-1}s^{-1}$ for the 6-membered ring nitroxides and $\approx 10^6$ $M^{-1}s^{-1}$ for the 5-membered ones. Therefore, having similar reduction potentials, the 6-membered ring nitroxides are better catalysts. Also, a better catalyst is a nitroxide having a lower reduction potential unless $RN^{+}=O$ is efficiently scavenged by reducing agents other than tyrosine and/or nitrite. The proposed mechanism further emphasizes the role of the reducing environment to the efficacy of nitroxide antioxidants.

Conflict of Interest

The authors declare that they have no conflicts of interest related to this work.

Funding

This work has been supported by the Pazy Foundation Grant number 276/19.

Appendix A. Supplementary data

References

[1] B. P. Soule, F. Hyodo, K. I. Matsumoto, N. L. Simone, J. A. Cook, M. C. Krishna, J. B. Mitchell, Therapeutic and clinical applications of nitroxide compounds, *Antioxid. Redox Signal.* **9** (2007) 1731-1743.

[2] B. P. Soule, F. Hyodo, K.-i. Matsumoto, N. L. Simone, J. A. Cook, M. C. Krishna, J. B. Mitchell, The chemistry and biology of nitroxide compounds, *Free Radic. Biol. Med.* **42** (2007) 1632-1650.

[3] C. S. Wilcox, Effects of tempol and redox-cycling nitroxides in models of oxidative stress, *Pharmacol. Ther.* **126** (2010) 119-145.

[4] E. Linares, L. V. Seixas, J. N. dos Prazeres, F. V. L. Ladd, A. A. B. L. Ladd, A. A. Coppi, O. Augusto, Tempol Moderately Extends Survival in a hSOD1G93A ALS Rat Model by Inhibiting Neuronal Cell Loss, Oxidative Damage and Levels of Non-Native hSOD1G93A Forms, *PLOS ONE* **8** (2013) e55868.

[5] M. Assayag, S. Goldstein, A. Samuni, N. Berkman, Cyclic nitroxide radicals attenuate inflammation and Hyper-responsiveness in a mouse model of allergic asthma, *Free Radic. Biol. Med.* **87** (2015) 148-156.

[6] A. Samuni, S. Goldstein, A. Russo, J. B. Mitchell, M. C. Krishna, P. Neta, Kinetics and mechanism of hydroxyl radical and OH-adduct radical reactions with nitroxides and with their hydroxylamines, *J. Am. Chem. Soc.* **124** (2002) 8719-8724.

[7] S. Goldstein, J. Lind, G. Merenyi, Reaction of organic peroxyl radicals with NO_2 and NO in aqueous solution: Intermediacy of organic peroxynitrate and peroxynitrite species, *J. Phys. Chem. A* **108** (2004) 1719-1725.

[8] S. Goldstein, A. Samuni, K. Hideg, G. Merenyi, Structure-activity relationship of cyclic nitroxides as SOD mimics and scavengers of nitrogen dioxide and carbonate radicals, *J. phys. Chem. A* **110** (2006) 3679-3685.

[9] S. Goldstein, A. Samuni, Kinetics and mechanism of peroxyl radical reactions with nitroxides: Inhibition of peroxyl radical-mediated enzyme inactivation., *J. Phys. Chem. A* **111** (2007) 1066-1072.

[10] K. D. Asmus, S. Nigam, R. L. Willson, Kinetics of nitroxyl radical reactions. A pulse-radiolysis conductivity study, *Int. J. Radiat. Biol. Relat. Stud. Phys. Chem. Med.* **29** (1976) 211-219.

[11] A. L. J. Beckwith, G. W. Evans, 25. Reactions of alkoxy-radicals. Part III. Formation of esters from alkyl nitrites, *J. Chem. Soc.* (1962) 130-137.

[12] S. Goldstein, A. Samuni, G. Merenyi, Kinetics of the reaction between nitroxide and thiyl radicals: Nitroxides as antioxidants in the presence of thiols, *J. Phys. Chem. A* **112** (2008) 8600-8605.

[13] C. Houee-Levin, K. Bobrowski, L. Horakova, B. Karademir, C. Schoneich, M. J. Davies, C. M. Spickett, Exploring oxidative modifications of tyrosine: An update on mechanisms of formation, advances in analysis and biological consequences, *Free Radic. Res.* **49** (2015) 347-373.

[14] F. Leinisch, M. Mariotti, M. Rykaer, C. Lopez-Alarcon, P. Hൣgglund, M. J. Davies, Peroxyl radical- and photo-oxidation of glucose 6-phosphate dehydrogenase generates cross-links and functional changes via oxidation of tyrosine and tryptophan residues, *Free Radic. Biol. Med.* **112** (2017) 240-252.

[15] H. Ischiropoulos, Biological tyrosine nitration: A pathophysiological function of nitric oxide and reactive oxygen species, *Arch. Biochem. Biophy.* **356** (1998) 1-11.

[16] R. Radi, Nitric oxide, oxidants, and protein tyrosine nitration, *Proc. Natl. Acad. Sci. U. S. A.* **101** (2004) 4003-4008.

[17] M. A. Lam, D. I. Pattison, S. E. Bottle, D. J. Keddie, M. J. Davies, Nitric Oxide and Nitroxides Can Act as Efficient Scavengers of Protein-Derived Free Radicals, *Chem. Res. Toxicol.* **21** (2008) 2111-2119.

[18] D. I. Pattison, M. Lam, S. S. Shinde, R. F. Anderson, M. J. Davies, The nitroxide TEMPO is an efficient scavenger of protein radicals: Cellular and kinetic studies, *Free Radic. Biol. Med.* **53** (2012) 1664-1674.

[19] S. M. Vaz, O. Augusto, Inhibition of myeloperoxidase-mediated protein nitration by tempol: Kinetics, mechanism, and implications, *Proc. Natl. Acad. Sci.U.S.A.* **105** (2008) 8191-8196.

[20] A. Samuni, E. Maimon, S. Goldstein, Nitroxides catalytically inhibit nitrite oxidation and heme inactivation induced by H2O2, nitrite and metmyoglobin or methemoglobin, *Free Rad. Biol. Med.* **101** (2016) 491-499.

[21] A. Samuni, E. Maimon, S. Goldstein, Mechanism of HRP-catalyzed nitrite oxidation by H_2O_2 revisited: Effect of nitroxides on enzyme inactivation and its catalytic activity, *Free Radic. Biol. Med.* **108** (2017) 832-839.

[22] S. Goldstein, A. Samuni, A. Russo, Reaction of cyclic nitroxides with nitrogen dioxide: The intermediacy of the oxoammonium cations, *J. Am. Chem. Soc.* **125** (2003) 8364-8370.

[23] N. V. Klassen, D. Marchington, H. C. E. McGowan, H_2O_2 determination by the I_3^- method and by $KMnO_4$ titration, *Anal. Chem.* **66** (1994) 2921-2925.

[24] K. G. Paul, T. Stigbrand, Four isoperoxidases from horse radish root, *Acta Chem. Scand.* **24** (1970) 3607-3617.

[25] T. Odajima, I. Yamazaki, Myeloperoxidase of the leukocyte of normal blood. I. Reaction of myeloperoxidase with hydrogen peroxide, *Biochim. Biophys. Acta - Enzymology* **206** (1970) 71-77.

[26] S. J. Klebanoff, A. Waltersdorph, H. Rosen, Antimicrobial activity of myeloperoxidase, *Methods Enzymol.* **105** (1984) 399-403.

[27] A. J. Gross, I. W. Sizer, Oxidation of tyramine and tyrosine by peroxidase, *J. Biol. Chem.* **234** (1959) 1611-1614.

[28] S. S. Lehrer, G. D. Fasman, Ultraviolet Irradiation Effects in Poly-L-tyrosine and Model Compounds. Identification of Bityrosine as a Photoproduct, *Biochem.* **6** (1967) 757-767.

[29] G. S. Bayse, A. W. Michaels, M. Morrison, Peroxidase-catalyzed oxidation of tyrosine, *Biochim. Biophys. Acta-Gen. Subj.* **284** (1972) 34-&.

[30] M. Valoti, K. F. Tipton, G. P. Sgaragli, Oxidative ring-coupling of tyrosine and its derivatives by purified rat intestinal peroxidase, *Biochem. Pharmacol.* **43** (1992) 945-951.

[31] S. Sakura, D. Fujimoto, Absorption and fluoresence study of tyrosine-derived crosslinking amino acids from collagen, *Photochem. Photobiol.* **40** (1984) 731-734.

[32] J. S. Jacob, D. P. Cistola, F. F. Hsu, S. Muzaffar, D. M. Mueller, S. L. Hazen, J. W. Heinecke, Human phagocytes employ the myeloperoxidase-hydrogen peroxide system to synthesize dityrosine, trityrosine, pulcherosine, and Isodityrosine by a tyrosyl radical-dependent pathway, *J. Biol. Chem.* **271** (1996) 19950-19956.

[33] L. A. Marquez, H. B. Dunford, Kinetics of oxidation of tyrosine and dityrosine by myeloperoxidase compounds I and II - Implications for lipoprotein peroxidation studies, *J. Biol. Chem.* **270** (1995) 30434-30440.

[34] T. Michon, M. Chenu, N. Kellershon, M. Desmadril, J. Gueguen, Horseradish peroxidase oxidation of tyrosine-containing peptides and their subsequent polymerization: A kinetic study, *Biochem.* **36** (1997) 8504-8513.

[35] H. Ischiropoulos, L. Zhu, J. Chen, M. Tsai, J. C. Martin, C. D. Smith, J. S. Beckman, Peroxynitrite-mediated tyrosine nitration catalyzed by superoxide dismutase, *Arch. Biochem. Biophys.* **298** (1992) 431-437.

[36] R. Roman, H. B. Dunford, Studies on Horseradish-Peroxidase .12. Kinetic Study of Oxidation of Sulfite and Nitrite by Compounds I and II, *Can. J. Chem.-Rev. Can. Chim.* **51** (1973) 588-596.

[37] F. Jin, J. Leitich, C. von Sonntag, The superoxide radical reacts with tyrosine-derived phenoxyl radicals by addition rather than by electron transfer, *J. Chem. Soc. Perkin Trans. 2* (1993) 1583-1588.

[38] L. K. Folkes, M. Trujillo, S. Bartesaghi, R. Radi, P. Wardman, Kinetics of reduction of tyrosine phenoxyl radicals by glutathione, *Arch. Biochem. Biophys.* **506** (2011) 242-249.

[39] M. R. DeFelippis, C. P. Murthy, F. Broitman, D. Weinraub, M. Faraggi, M. H. Klapper, Electrochemical properties of tyrosine phenoxy and tryptophan indolyl radicals in peptides and amino acid analogs, *J. Phys. Chem.* **95** (1991) 3416-3419.

[40] R. B. Martin, J. T. Edsall, D. B. Wetlaufer, B. R. Hollingworth, A Complete Ionization Scheme for Tyrosine, and the Ionization Constants of Some Tyrosine Derivatives, *J. Biol. Chem.* **233** (1958) 1429-1435.

[41] S. Goldstein, G. Merenyi, A. Russo, A. Samuni, The role of oxoammonium cation in the SOD-Mimic activity of cyclic nitroxides, *J. Am. Chem. Soc.* **125** (2003) 789-795.

[42] M. Tien, Myeloperoxidase-catalyzed oxidation of tyrosine, *Arch. Biochem. Biophys.* **367** (1999) 61-66.

[43] A. Mahmoudi, K. Nazari, M. Khosraneh, B. Mohajerani, V. Kelay, A. A. Moosavi-Movahedi, Can amino acids protect horseradish peroxidase against its suicide-peroxide substrate?, *Enzyme Microbial Technol.* **43** (2008) 329-335.

[44] F. N. Pedron, S. Bartesaghi, D. o. A. Estrin, R. Radi, A. Zeida, A computational investigation of the reactions of tyrosyl, tryptophanyl, and cysteinyl radicals with nitric oxide and molecular oxygen, *Free Rad. Res.* **53** (2019) 18-25.

[45] W. A. Prutz, H. Monig, J. Butler, E. J. Land, Reactions of Nitrogen-Dioxide in Aqueous Model Systems - Oxidation of Tyrosine Units in Peptides and Proteins, *Arch. Biochem. Biophys.* **243** (1985) 125-134.

[46] Z. B. Alfassi, Selective oxidation of tyrosine - Oxidation by NO_2 and ClO_2 at basic pH, *Radiat. Phys. Chem.* **29** (1987) 405-406.

[47] S. Goldstein, G. Czapski, J. Lind, G. Merenyi, Tyrosine nitration by simultaneous generation of NO and $O_2^{\cdot -}$ under physiological conditions - How the radicals do the job, *J. Biol. Chem.* **275** (2000) 3031-3036.

[48] A. Samuni, E. Maimon, S. Goldstein, Nitroxides protect horseradish peroxidase from H_2O_2-induced inactivation and modulate its catalase-like activity, *Biochim. Biophys. Acta Gen. Subj*. **1861** (2017) 2060-2069.

[49] D. N. Dolman, G. A.; Thurlow, M. D.; Dunford, H. B., Kinetic study of reaction of horseradish-peroxidase with hydrogen-peroxide, *Can. J. Biochem*. **53** (1975) 495-501.

Highlights

- Nitroxides catalytically inhibit tyrosine oxidation mediated by peroxidase/H_2O_2.
- Nitroxide catalysts inhibit tyrosine nitration mediated by peroxidase/H_2O_2/nitrite.
- The inhibitory effect increases as nitroxide reduction potential decreases.
- The 6-membered ring nitroxides are better catalyst than the 5-memnbered ones.
- The proposed mechanism implies a role of reducing agents on nitroxide efficacy.

Graphical abstract